Supplementary Information

Mechanochromic polyurethane elastomers containing main-chain naphthalimide moieties

Tomoya Tada, Tetsuma Inaoka, Hiromitsu Sogawa and Fumio Sanda*

Faculty of Chemistry, Materials and Bioengineering, Kansai University

3-3-35 Yamate-cho, Suita, Osaka 564-8680, Japan

*Corresponding Author.
E-mail: sanda@kansai-u.ac.jp (F. Sanda)

Instruments

^{1}H (400 MHz) and ^{13}C (100 MHz) NMR spectra were measured in deuterated chloroform ($CDCl_3$), trifluoroacetic acid-*d* (TFA-*d*) or dimethyl sulfoxide-*d* (DMSO-d_6) on JEOL ECA-400, ECS-400 and ECZ-400 spectrometers. IR spectra were measured on a JASCO FT/IR-4100 spectrophotometer. Number-average molecular weight (M_n) and polydispersity ($Đ$) values of polymers were determined by size exclusion chromatography (SEC) eluted with LiBr solution (10 mM) in *N,N*-dimethylformamide (DMF) with a Shodex LF-804 column calibrated by polystyrene standards at 40 °C using JASCO SEC system consisting of RI-930, UV-4570, PU-4580, DG-2080-53, CO-965, LC-NetII/ADC. Dynamic light scattering (DLS) measurements were performed using a square glass cell on a Malvern Instruments Zetasizer Nano ZSP at 20 °C. TGA was acquired with a SHIMADZU thermogravimetric analyzer TGA-50 with a heating rate of 10 °C min^{-1} from 50 °C to 600 °C under nitrogen at a flow rate of 50 mL min^{-1}. UV–vis absorption spectra were recorded on a SHIMADZU UV-2600 spectrophotometer. Photoluminescence spectra and absolute quantum yields were measured on a SHIMADZU spectrofluorophotometer RF-6000. Fluorescence lifetimes of solution samples were measured in a 4-sided quartz cell on a HORIBA DeltaFlex Lifetime System equipped with a NanoLED-405 (λ_{ex} = 405 nm). Lap shear test was performed on a SHIMADZU EZ-LX.

Reagents

4-Bromo-1,8-naphthalic anhydride (TCI), 6-amino-1-hexanol (TCI), trimethylsilylacetylene (Apollo Scientific Ltd.), 1,4-butanediol (BD, TCI), 1,4-diiodobenzene (TCI), diisopropylamine (TCI), CuI (NACALAI TESQUE, INC.), polytetrahydrofuran 2000 (PTHF, FUJIFILM Wako Pure Chemical), methylenediphenyl 4,4'-diisocyanate (MDI, FUJIFILM Wako Pure Chemical) and dibutyltin dilaurate (DBTDL, TCI) were purchased and used without purification. $PdCl_2(PPh_3)_2$ was synthesized according to the literature.[S1] Solvents used in the reactions under Ar were dehydrated over molecular sieves 4A1/16 and degassed by Ar bubbling before use.

Synthesis of monomer 1

Compound 2

A mixture of 4-bromo-1,8-naphthalic anhydride (5.00 g, 18.0 mmol), 6-amino-1-hexanol (2.53 g, 21.6 mmol) and EtOH (100 mL) was stirred at 80 °C for 18 h. After cooling the reaction mixture to r.t., it was slowly poured into water (300 mL) to precipitate a solid. It was collected by filtration, and dried under reduced pressure to obtain **2** (6.0 g, 15.9 mmol, 88%) as yellow solid. ^{1}H NMR (400 MHz, $CDCl_3$): δ 8.65 (dd, J = 1.2, 0.8 Hz, 1H), 8.56 (dd, J = 1.2, 0.8 Hz, 1H), 8.42 (d, J = 8.0 Hz, 1H), 8.05 (d, J = 8.0 Hz, 1H), 7.84 (t, J = 7.6 Hz, 1H), 4.17 (t, J = 8.0 Hz, 2H), 3.64 (broad s, 2H), 1.79–1.37 (m, 8H).

Compound 3

A mixture of **2** (2.0 g, 4.5 mmol), trimethylsilylacetylene (0.95 mL, 6.8 mmol), $PdCl_2(PPh_3)_2$ (9.5 mg, 0.013 mmol), CuI (2.6 mg, 0.013 mmol), PPh_3 (3.6 mg, 0.013 mmol), Et_3N (15 mL) and THF (30 mL) was stirred under Ar at 80 °C for 18 h. After cooling the reaction mixture to r.t., solvents were evaporated off. $CHCl_3$ was added to the residue, and the resultant solution was washed with saturated aq. NH_4Cl. The organic layer was separated and dried over $MgSO_4$, and concentrated on a rotary evaporator. The residual mass was purified by silica gel column chromatography (eluent: hexane/ethyl acetate = 1/1, v/v) to obtain compound **3** (1.60 g, 4.07 mmol, 90%) as a yellow solid. ^{1}H NMR (400 MHz, $CDCl_3$) δ 8.63–8.61 (m, 2H), 8.52 (d, J = 7.6, 1H), 7.90 (d, J = 7.6 Hz, 1H), 7.81 (t, J = 7.6 Hz, 1H), 4.17 (t, J = 7.6 Hz, 2H), 3.64 (t, J = 6.4 Hz, 2H), 1.75–1.45 (m, 8H), 0.37 (s, 9H).

Compound 4

A mixture of **3** (1.57 g, 3.99 mmol), K_2CO_3 (1.00 g, 7.23 mmol) and MeOH (50 mL) was stirred at r.t. for 2 h. Then, the reaction mixture was slowly poured into water (300 mL) to precipitate a solid. It was separated by filtration, and dried under reduced pressure. The crude product was purified by silica gel column chromatography (eluent: hexane/ethyl acetate = 2/3 v/v) to obtain **4** (0.30 g, 0.93 mmol, 23%) as a pale-yellow solid. ^{1}H NMR (400 MHz, $CDCl_3$) δ 8.65 (dd, J = 13.0 Hz, 7.8 Hz, 2H), 8.53 (d, J = 7.7 Hz, 1H), 7.94 (d, J = 7.7 Hz, 1H), 7.83 (dd, J = 8.4, 7.5 Hz, 1H), 4.20–4.16 (m, 2H), 3.64 (q, J = 5.9 Hz, 2H), 1.80–1.72 (m, 2H), 1.63–1.57 (m, 4H), 1.50–1.37 (m, 5H).

Monomer 1

A mixture of compound **4** (0.200 g, 0.622 mmol), 1,4-diiodobenzene (0.0825 g, 0.250 mmol), $PdCl_2(PPh_3)_2$ (5.26 mg, 7.50 μmol), CuI (0.14 mg, 7.5 μmol), PPh_3 (0.20 mg, 7.5 μmol), iPr$_2$NH (1 mL) and THF (10 mL) was stirred under Ar at r.t. for 18 h. After that, a precipitated solid was separated by filtration, and dried under reduced pressure to obtain **1** (0.176 g, 0.246 mmol, 98%) as a yellow solid. ^{1}H NMR (400 MHz, TFA-d) δ 8.95–8.68 (broad, 6H), 8.05–7.96 (broad, 4H), 7.73 (s, 4H), 4.49–4.44 (broad, 4H), 3.99–3.90 (broad, 4H), 2.04–1.56 (broad, 16H).

Synthesis of polymers

Poly-1

DBTDL (1 mol%) was added to a stirred mixture of compound **1**, PTHF (M_n = 2,000), and MDI in THF and the mixture was stirred at 70 °C for 3 h. A solution of BD in THF (10 mL) was then added and the reaction mixture was stirred at 70 °C for an additional 24 h. MeOH (1 mL) was added to the reaction mixture and after stirring for another 30 min the reaction mixture was poured into H_2O (300 mL). The precipitate was filtered off and dried *in vacuo* at r.t. for 24 h to obtain poly-**1** as a yellow rubbery solid.

Poly-2 and poly-2-1

Poly-**2** was synthesized in a manner similar to poly-**1**, without adding **1**. Poly-**2-1** was prepared by mixing poly-**2** (0.375 g) and **1** (0.83 mg) in THF, followed by volatilization of THF.

Preparation of polyurethane films

Typical Procedure. A solution of poly-**1** (375 mg) in THF (7.5 mL) was poured into a petri dish (radius: 30 mm). It was covered with an inverted funnel to evaporate THF slowly for a period of 24 h. The resulting film was further dried *in vacuo* at r.t. overnight.

Computation

QM calculations were performed with the Gaussian 16,[S2] Rev C.01, using the DFT method with ωB97XD functional in conjunction with 6-31G* basis set, running on the supercomputer system Fugaku provided by the RIKEN Center for Computational Science and Research Center for Computational Science, Okazaki, Japan. The UV–vis absorption and fluorescence spectra were simulated by the TD-DFT method, and analyzed using GaussView 6. [S3] The simulated CD/UV–vis absorption spectra, and geometry-optimized structures were illustrated using GaussView 6 and PyMOL,[S4] respectively. Noncovalent interactions[S5] were indicated by the reduced density gradient isosurfaces generated by Multiwfn[S6,S7] based on the PROAIMS wavefunction calculated by Gaussian and visualized by PyMOL. MD simulations were performed with LAMMPS 2020.[S8] The initial structures for MD simulations were constructed using the Winmostar V11, X-Ability Co. Ltd., Tokyo, Japan. Solvent boxes were constructed using PACKMOL.[S9] The general amber force field (GAFF) was used.[S10,S11] Atomic charges were assigned using a restrained electrostatic potential (RESP) fit mode[S12,S13] with calculations performed at the HF/6-31G* level using Gaussian 16. The long-range Coulomb interactions were calculated using the smooth particle mesh Ewald (SPME) method.[S14] A long-range correction of the LJ potential was applied to the energy and pressure. The MD trajectories were analyzed using CPPTRAJ,[S15] and the snapshots were taken using OVITO.[S16]

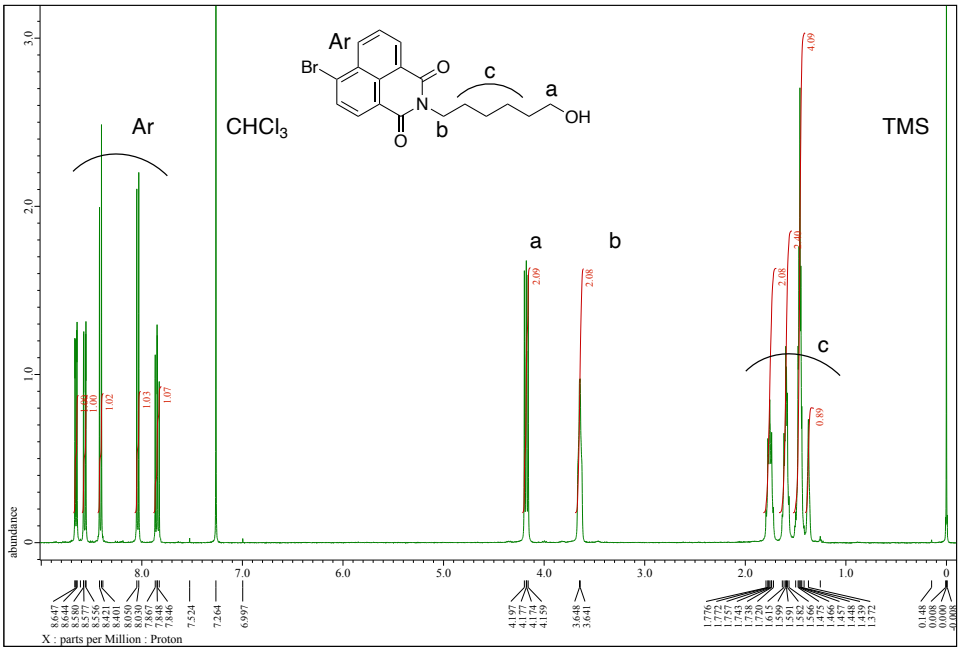

Fig. S1 ^{1}H NMR (400 MHz) spectrum of **2** measured in $CDCl_3$.

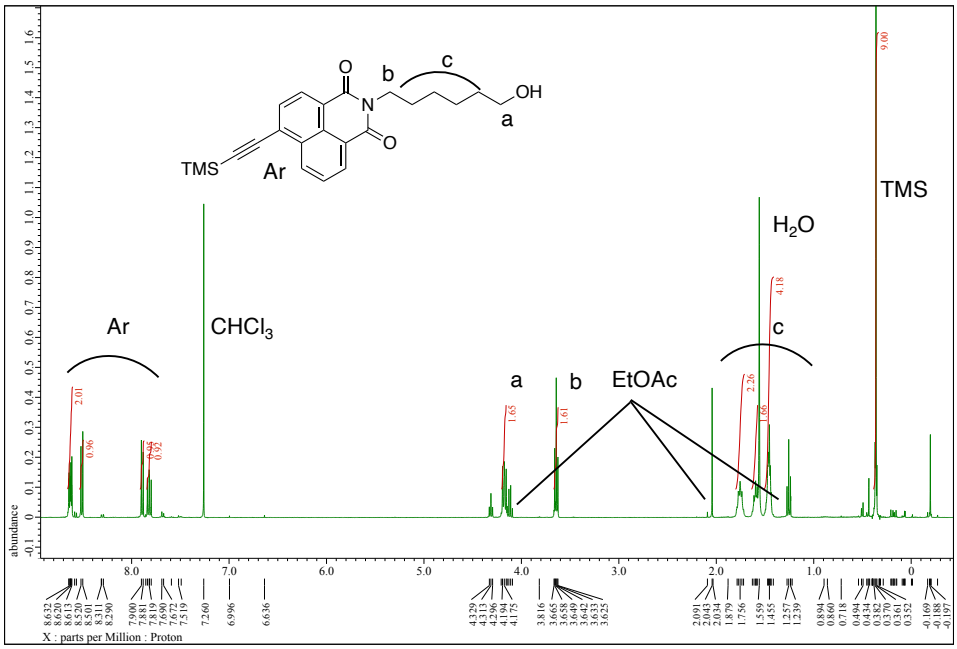

Fig. S2 ^{1}H NMR (400 MHz) spectrum of **3** measured in $CDCl_3$.

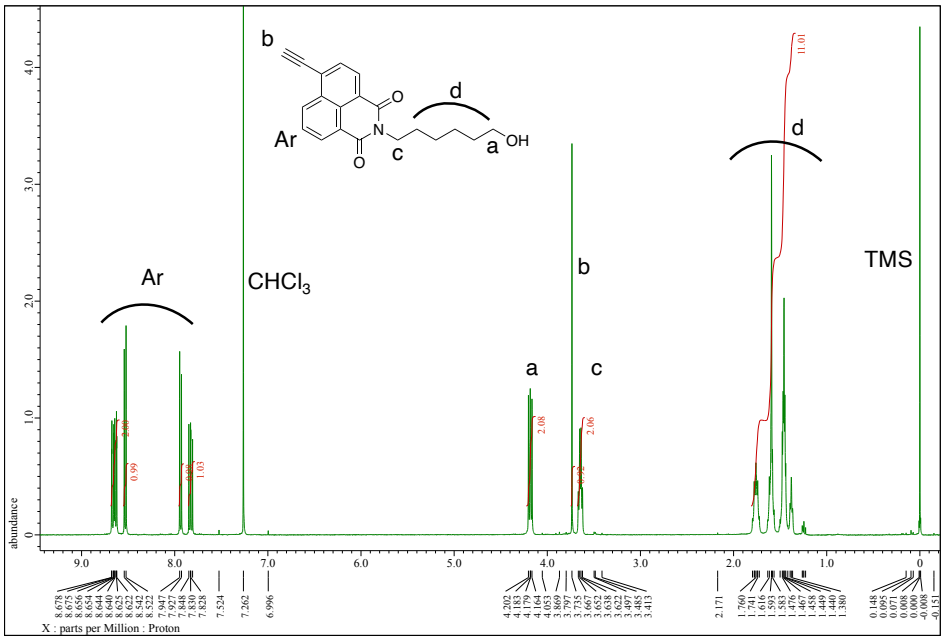

Fig. S3 ^{1}H NMR (400 MHz) spectrum of **4** measured in $CDCl_3$.

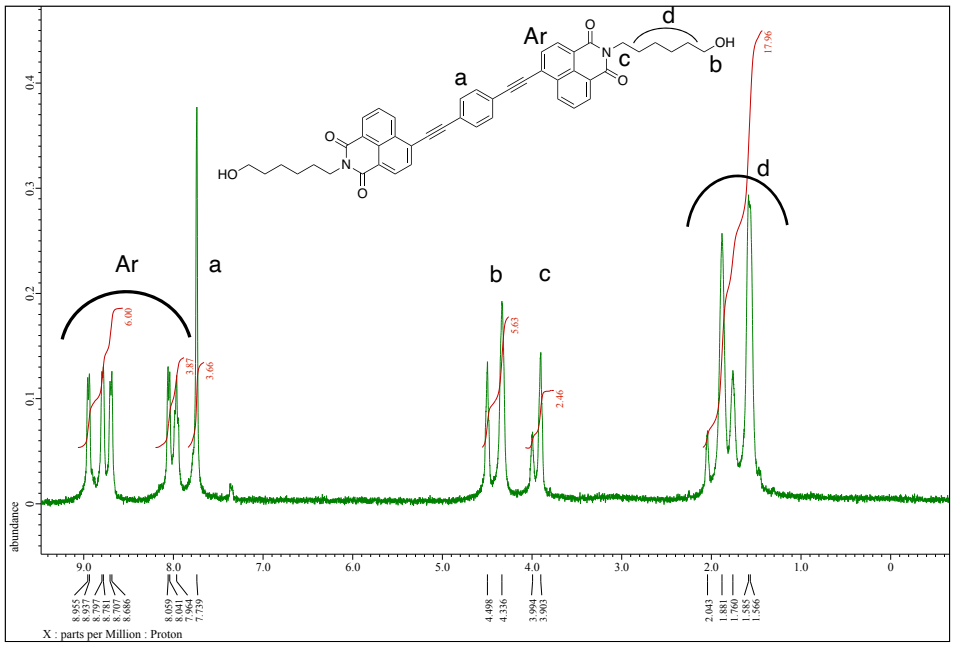

Fig. S4 ^{1}H NMR (400 MHz) spectrum of **1** measured in TFA-*d*.

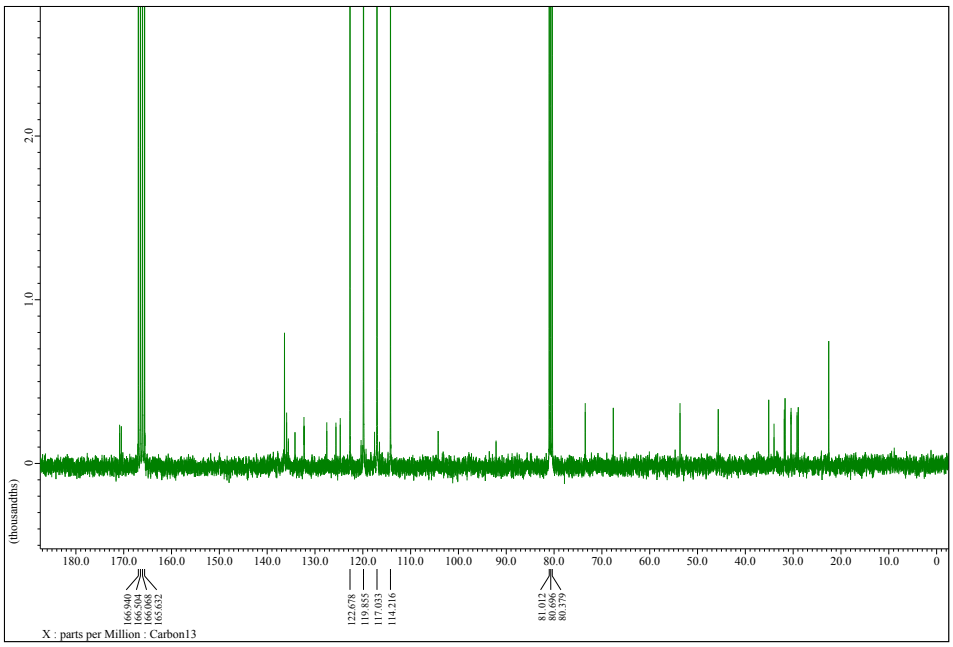

Fig. S5 ^{13}C NMR (400 MHz) spectrum of **1** measured in TFA-*d*.

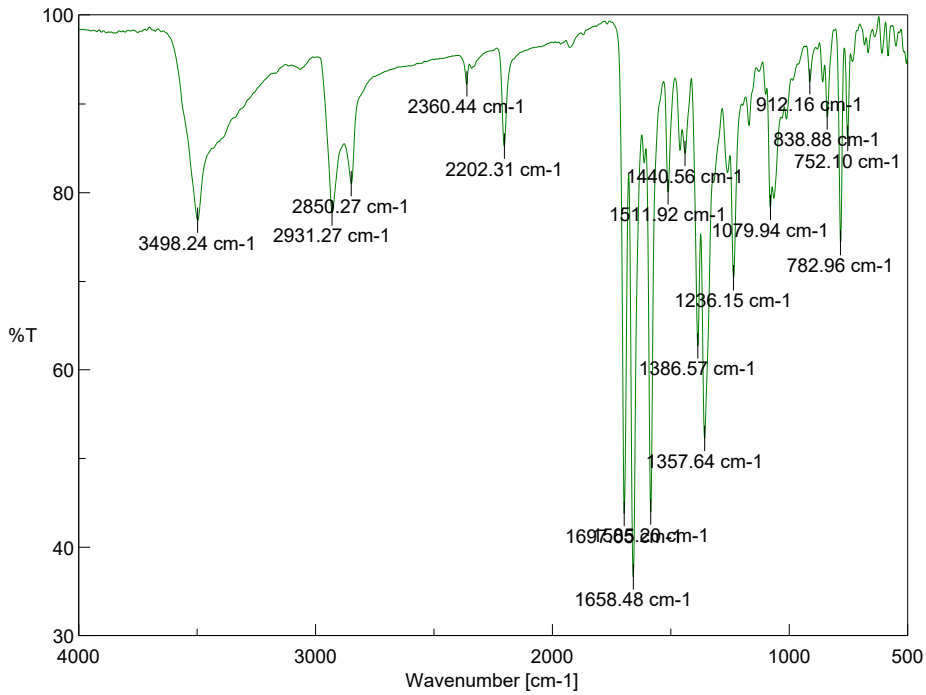

Fig. S6 IR spectrum of **1** measured by the KBr pellet method.

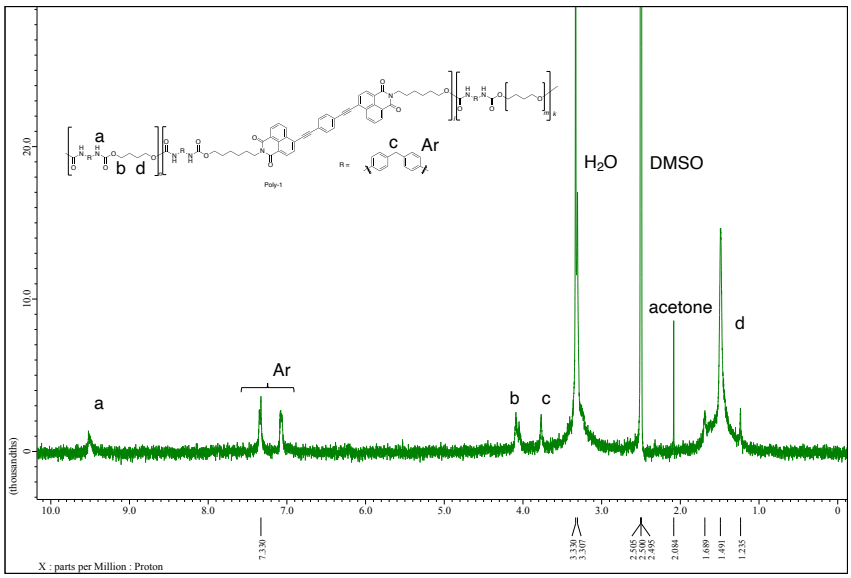

Fig. S7 ^{1}H NMR (400 MHz) spectrum of poly-**1**$_{0.3}$ measured in DMSO-d_6.

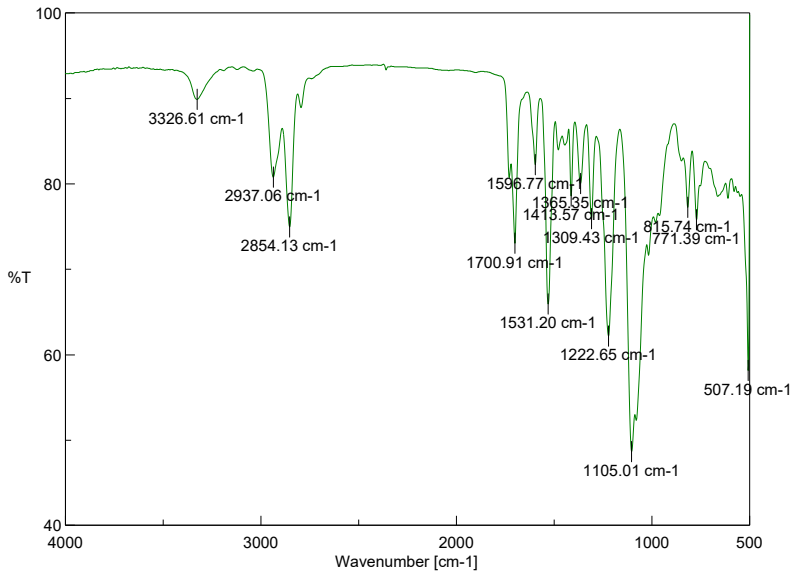

Fig. S8 IR spectrum of poly-**1**$_{0.3}$ measured by the KBr pellet method.

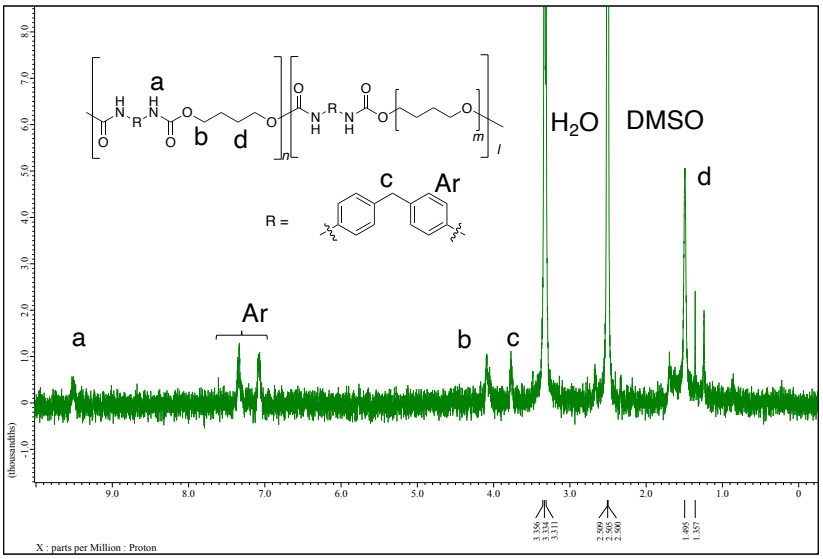

Fig. S9 ^{1}H NMR (400 MHz) spectrum of poly-**2**-**1**$_{0.3}$ measured in DMSO-d_6.

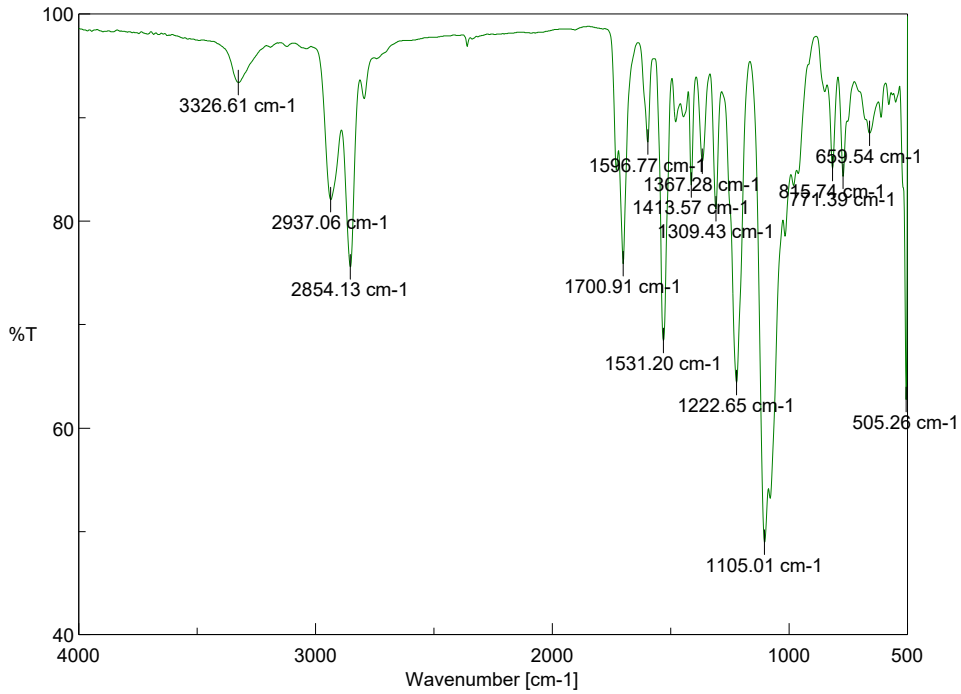

Fig. S10 IR spectrum of poly-**2**-**1**$_{0.3}$ measured by the KBr pellet method.

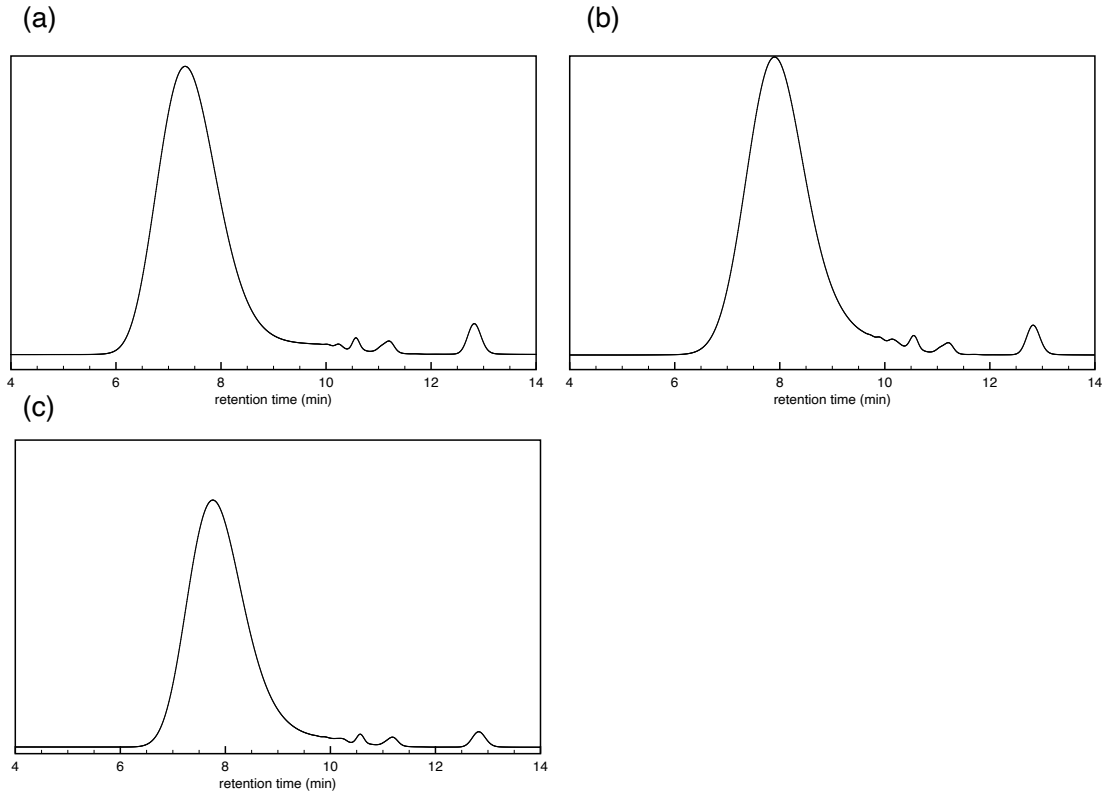

Fig. S11 SEC charts of (a) poly-$\mathbf{1}_{0.1}$, (b) poly-$\mathbf{1}_{0.3}$ and (c) poly-$\mathbf{2}$-$\mathbf{1}_{0.3}$ (eluent: THF).

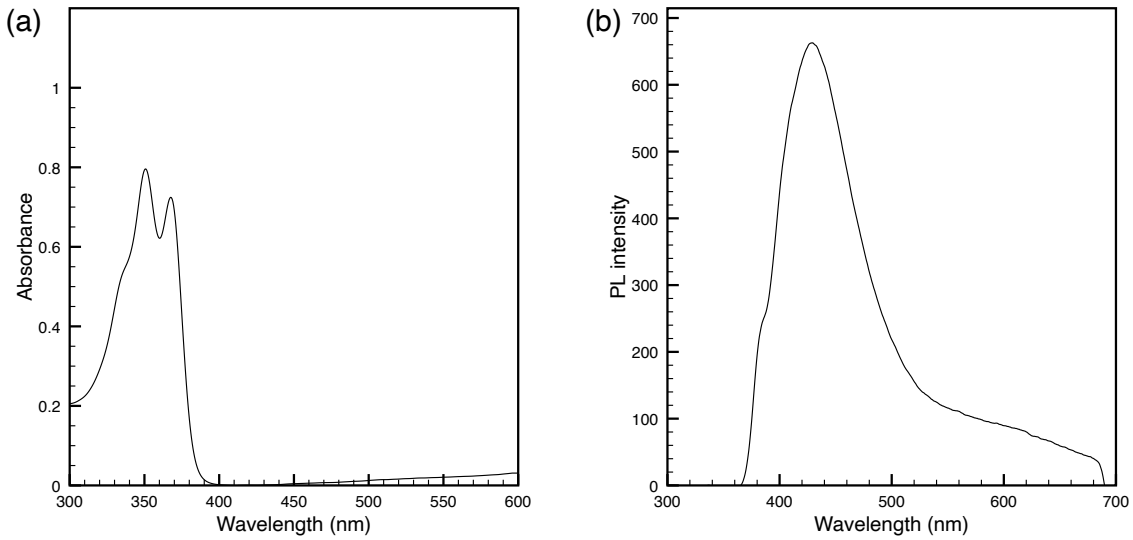

Fig. S12 (a) UV–vis absorption spectrum of **4** measured in NMP (c = 0.05 mM) and (b) PL spectrum of **4** excited at 351 nm measured in NMP (c = 0.05 mM).

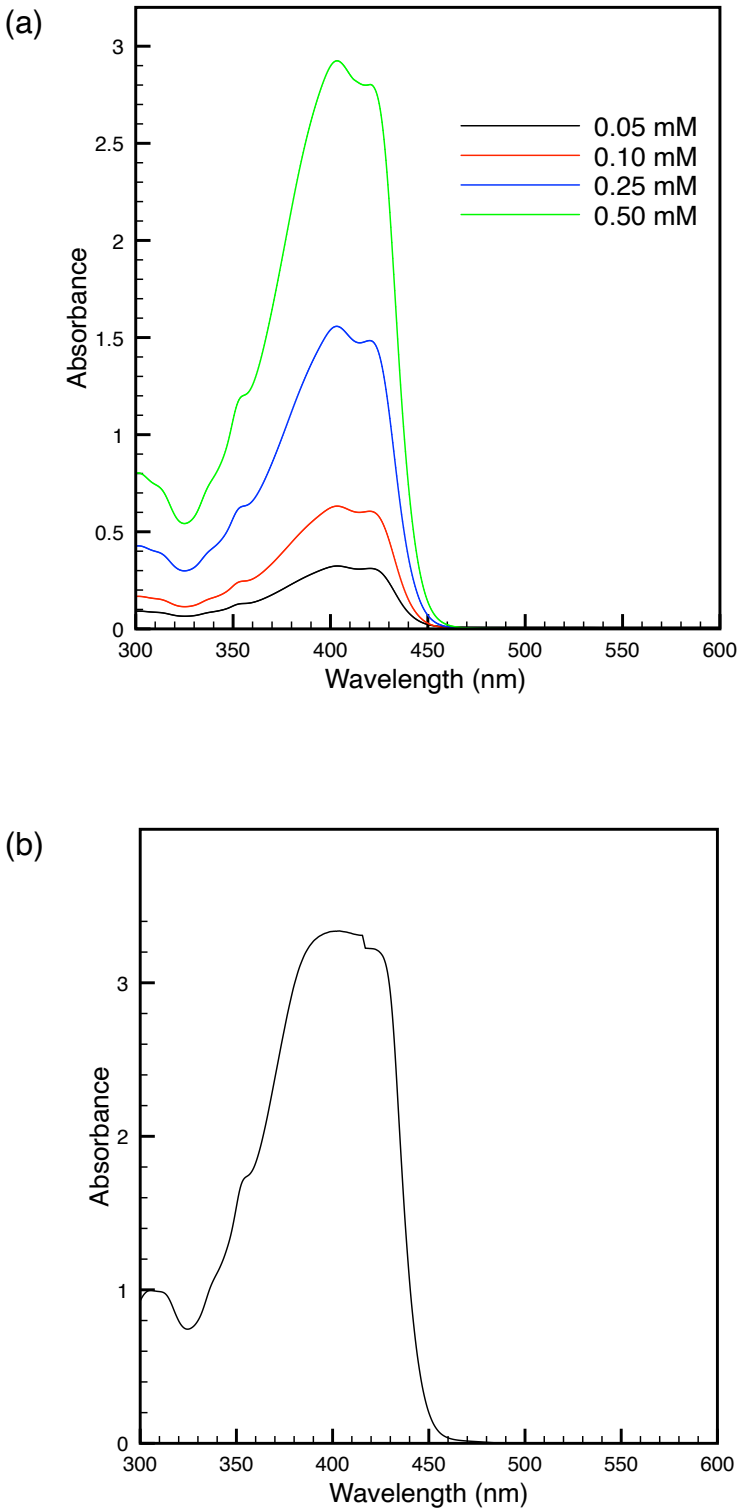

Fig. S13 (a) Non-normalized UV–vis absorption spectra of **1** measured in NMP (c = 0.05–0.50 mM), corresponding to Fig. 1a. (b) UV–vis absorption spectrum of **1** measured in NMP (c = 0.80 mM), showing saturation of the absorbance.

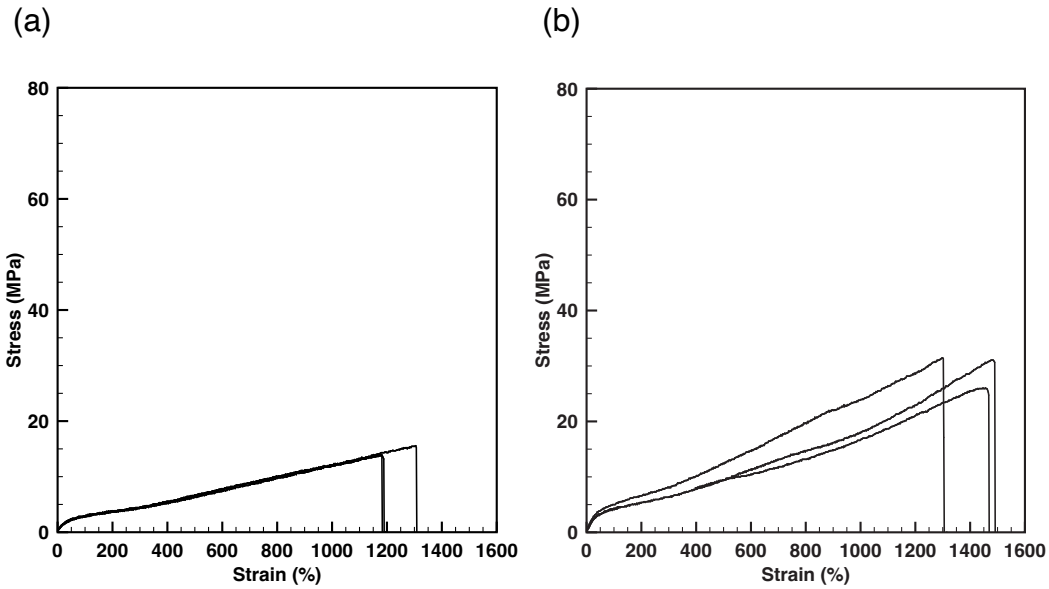

Fig. S14 Stress-strain curves of (a) poly-**1**$_{0.3}$ and (c) poly-**2-1**$_{0.3}$ films. Each curve shows data obtained from three different specimens. The experiments were conducted with a strain rate of 10 mm/min at r.t.

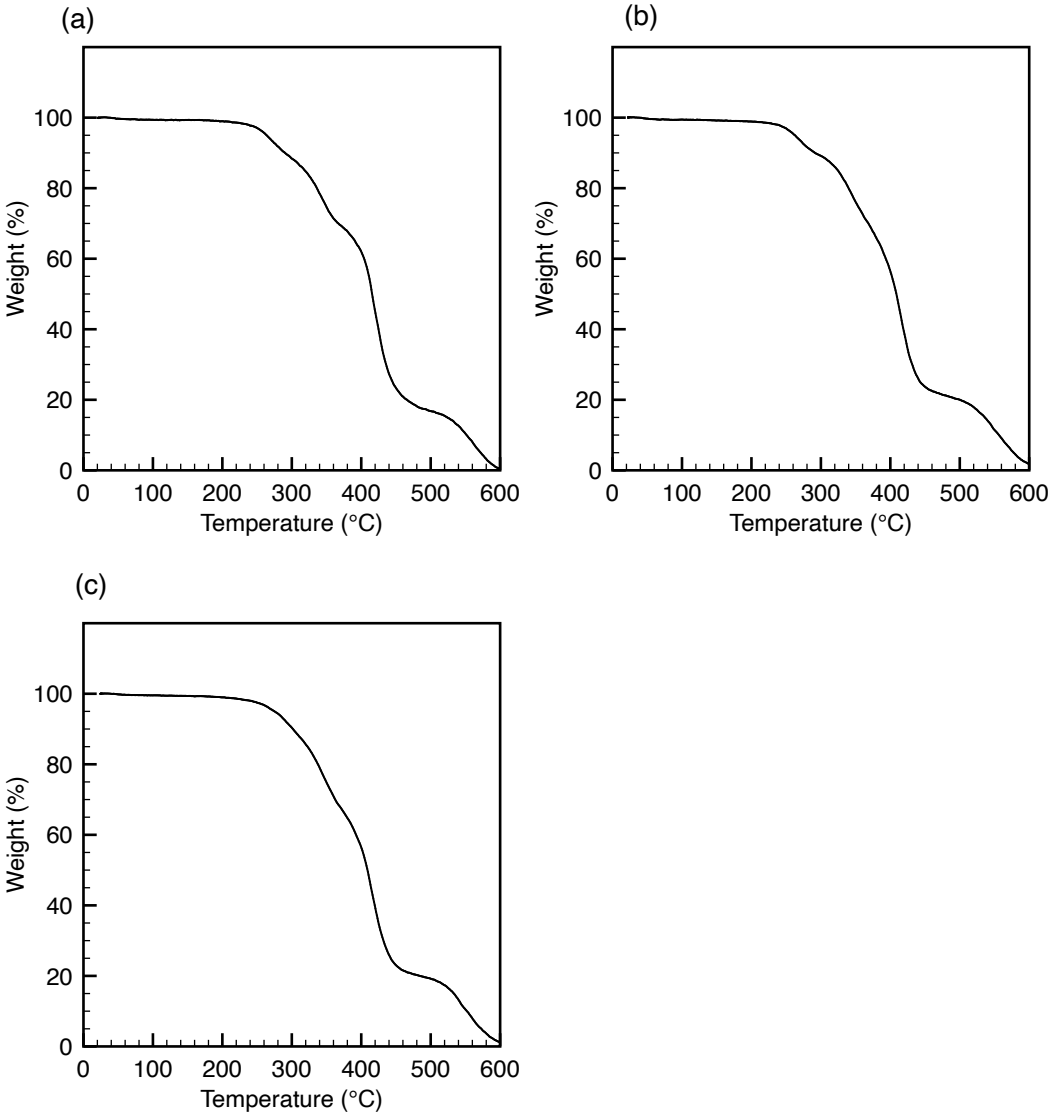

Fig. S15 TGA traces of (a) poly-**1**$_{0.1}$, (b) poly-**1**$_{0.1}$ and (c) poly-**2-1**$_{0.3}$ measured at a heating rate of 10 °C/min under N_2.

Table S1 5% and 10% weight loss temperatures of the polymers [a]

polyurethane	T_{d5} (°C)	T_{d10} (°C)
poly-**1**$_{0.1}$	263	290
poly-**1**$_{0.3}$	260	290
poly-**2-1**$_{0.3}$	275	301

[a] Determined by TGA under N_2 at a heating rate of 10 °C/min.

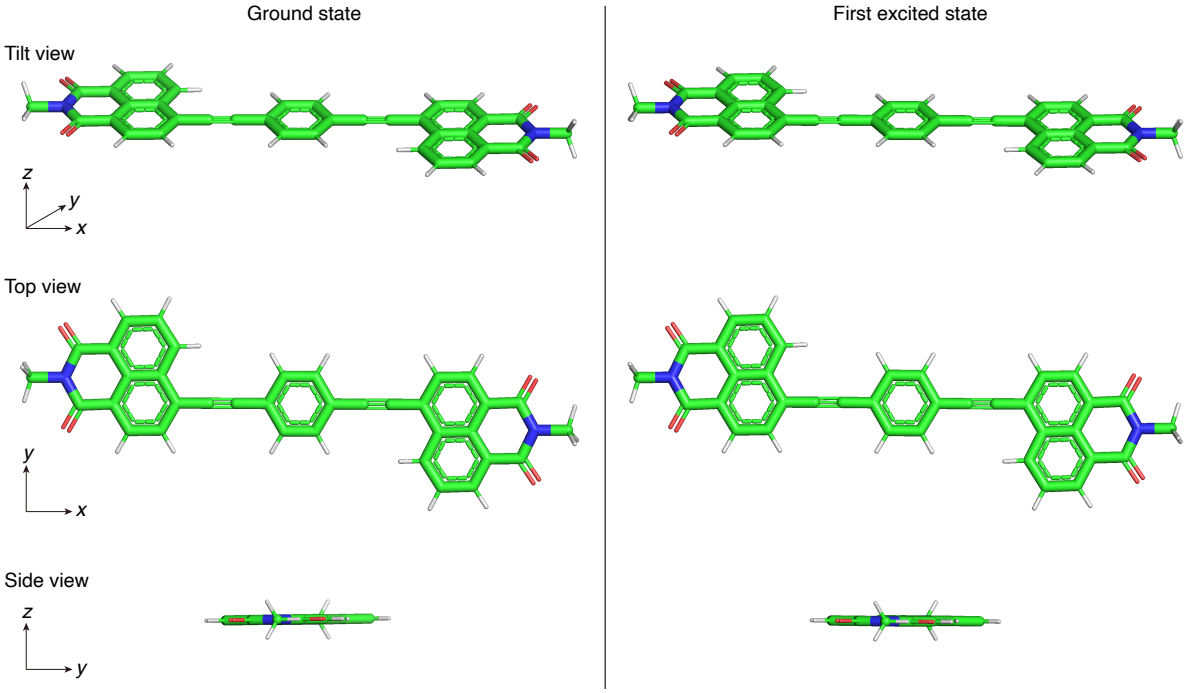

Fig. S16 Conformers of monomer models of **1** at the ground state (left) and first excited state (right). At the ground state, the geometries were optimized by the DFT method (ωB97XD/6-31G*). At the first excited state, the geometries were optimized by the TD-DFT method (ωB97XD/6-31G*) starting from the geometries optimized at the ground state.

References

S1 A. Naghipour, A. Ghorbani-Choghamarani, H. Babaee, M. Hashemi and B. Notash, Crystal structure of a novel polymorph of trans-dichlorobis(triphenylphosphine)palladium(II) and its application as a novel, efficient and retrievable catalyst for the amination of aryl halides and Stille cross-coupling reactions, *J. Organomet. Chem.,* 2017, **841**, 31–38. https://doi.org/10.1016/j.jorganchem.2016.10.002

S2 M. J. Frisch, G. W. Trucks, H. B. Schlegel, G. E. Scuseria, M. A. Robb, J. R. Cheeseman, G. Scalmani, V. Barone, G. A. Petersson, H. Nakatsuji, X. Li, M. Caricato, A. V. Marenich, J. Bloino, B. G. Janesko, R. Gomperts, B. Mennucci, H. P. Hratchian, J. V. Ortiz, A. F. Izmaylov, J. L. Sonnenberg, D. Williams-Young, F. Ding, F. Lipparini, F. Egidi, J. Goings, B. Peng, A. Petrone, T. Henderson, D. Ranasinghe, V. G. Zakrzewski, J. Gao, N. Rega, G. Zheng, W. Liang, M. Hada, M. Ehara, K. Toyota, R. Fukuda, J. Hasegawa, M. Ishida, T. Nakajima, Y. Honda, O. Kitao, H. Nakai, T. Vreven, K. Throssell, J. A. Montgomery, Jr., J. E. Peralta, F. Ogliaro, M. J. Bearpark, J. J. Heyd, E. N. Brothers, K. N. Kudin, V. N. Staroverov, T. A. Keith, R. Kobayashi, J. Normand, K. Raghavachari, A. P. Rendell, J. C. Burant, S. S. Iyengar, J. Tomasi, M. Cossi, J. M. Millam, M. Klene, C. Adamo, R. Cammi, J. W. Ochterski, R. L. Martin, K. Morokuma, O. Farkas, J. B. Foresman and D. J. Fox, Gaussian, Inc., Wallingford CT, 2016.

S3 GaussView, Version 6, R. Dennington, T. A. Keith and J. M. Millam, Semichem Inc., Shawnee Mission, KS, 2016.

S4 L. Schrödinger and W. L. DeLano, PyMOL 2020, Available from: https://www.pymol.org/pymol

S5 E. R. Johnson, S. Keinan, P. Mori-Sánchez, J. Contreras-García, A. J. Cohen and W. Yang, Revealing Noncovalent Interactions, *J. Am. Chem. Soc.*, 2010, **132**, 6498–6506. https://doi.org/10.1021/ja100936w

S6 T. Lu and F. Chen, Multiwfn: A Multifunctional Wavefunction Analyzer, *J. Comput. Chem.* **2012**, *33*, 580–592. https://doi.org/10.1002/jcc.22885

S7 T. Lu, A comprehensive electron wavefunction analysis toolbox for chemists, Multiwfn. *J. Chem. Phys.*, 2024, **161**, 082503. https://doi.org/10.1063/5.0216272

S8 A. P. Thompson, H. M. Aktulga, R. Berger, D. S. Bolintineanu, W. M. Brown, P. S. Crozier, P. J. in't Veld, A. Kohlmeyer, S. G.Moore, T. D. Nguyen, R. Shan, M. J. Stevens, J. Tranchida, C. Trott and S. J. Plimpton, LAMMPS - A Flexible Simulation Tool for Particle-Based Materials Modeling at the Atomic, Meso, and Continuum Scales, *Comput. Phys. Commun.*, 2022, **271**, 108171. https://doi.org/10.1016/j.cpc.2021.108171

S9 L. Martínez, R. Andrade, E. G. Birgin, J. M. Martínez, PACKMOL: A Package for Building Initial Configurations for Molecular Dynamics Simulations, *J. Comput. Chem.*, 2009, **30**, 2157–2164. https://doi.org/10.1002/jcc.21224

S10 J. Wang, R. M. Wolf, J. W. Caldwell, P. A. KollmanCase, Development and testing of a general AMBER force field, *J. Comp. Chem.* **2004**, *25*, 1157–1174. https://doi.org/10.1002/jcc.20035

S11 J. Wang, W. Wang, P. A. Kollman and D. A. Case, Automatic atom type and bond type perception in molecular mechanical calculations. *J. Mol. Graph. Model.* **2006**, *25*, 247260. https://doi.org/10.1016/j.jmgm.2005.12.005

S12 C. I. Bayly, P. Cieplak, W. Cornell and P. A. Kollman, A Well-Behaved Electrostatic Potential Based Method Using Charge Restraints for Deriving Atomic Charges: The RESP Model, *J. Phys. Chem.*, 1993, **97**, 10269–10280. https://doi.org/10.1021/j100142a004

S13 W. D. Cornell, P. Cieplak, C. I. Bayly, I. R. Gould, K. M. Merz, D. M. Ferguson, D. C. Spellmeyer, T. Fox, J. W. Caldwell and P. A. Kollman, A Second Generation Force Field for the Simulation of Proteins, Nucleic Acids, and Organic Molecules, *J. Am. Chem. Soc.*, 1995, **117**, 5179–5197. https://doi.org/10.1021/ja955032e

S14 U. Essmann, L.Perera, M. L. Berkowitz, T. Darden, H. Lee and L. G. Pedersen, A Smooth Particle Mesh Ewald Method, *J. Chem. Phys.*, 1995, **103**, 8577–8593. https://doi.org/10.1063/1.470117

S15 D. R. Roe and T. E. Cheatham III, PTRAJ and CPPTRAJ: Software for Processing and Analysis of Molecular Dynamics Trajectory, *J. Chem. Theory Comput.*, 2013, **9**, 3084–3095. https://doi.org/10.1021/ct400341p

S16 A. Stukowski, Visualization and analysis of atomistic simulation data with OVITO–the Open Visualization Tool, *Modelling Simul. Mater. Sci. Eng.*, 2010, **18**, 015012. https://doi.org/10.1088/0965-0393/18/1/015012